Morphology And Effective Refractive Indices Of Aerosols Emitted From High-Moisture-Content Biomass Combustion

Rajan K. Chakrabarty, [1,2,*] Lung-Wen Antony Chen, [2] Hans Moosmüller, [2] Claudio Mazzoleni, [3] Petr Chylek, [3] Manvendra Dubey, [3] W.Patrick Arnott, [4] Kristin Lewis, [4] and Wei Min Hao[5]

[1] *Chemical Physics Program, University of Nevada Reno, Reno, Nevada – 89557, USA*

[2] *Division of Atmospheric Sciences, Desert Research Institute, Reno, Nevada – 89512, USA*

[3] *Geochemistry and Climate Focus Team, Los Alamos National Laboratory, New Mexico – 87545, USA*

[4] *Department of Physics, University of Nevada Reno, Reno, Nevada -89557, USA*

[5] *USDA Forest Service, Rocky Mountain Research Station, Fire Sciences Laboratory, Missoula, Montana, USA.*

USFS, Missoula, MT, USA

Fire Pit with Hood, Stack to study change in particle properties with phase of fire and time

11/16/2003- 11/23/2003

5/25/2006-6/10/2006

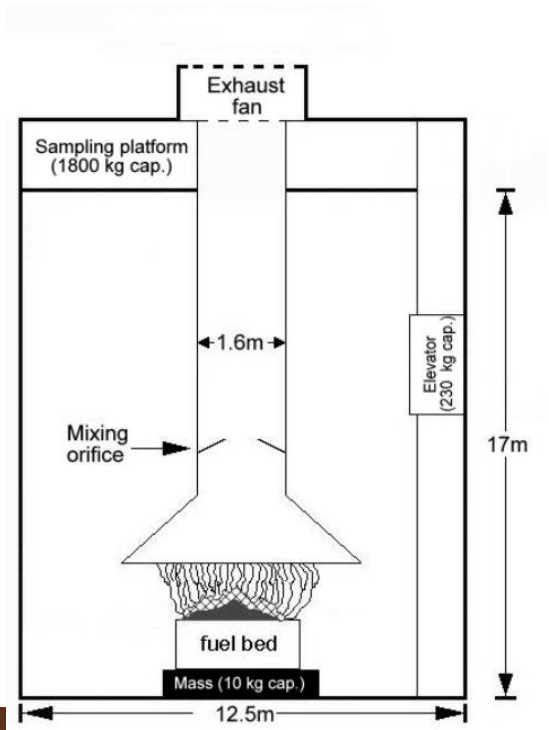

Chamber Burn

Sealed Chamber room with approx. volume of 3,300 m^3 to study evolution of particle in long Residence time

Wildland fire emissions impact air quality (PM, CO, NO_x, O_3), visibility, and climate

- Incomplete combustion Results in Gases and **Carbonaceous Particles**

- Carbonaceous Particles consist mostly of Elemental Carbon (**EC**) and Organic Carbon (**OC**)

- **EC** is **Black (Scattering & Absorbing)** and **Thermally Refractive**

- **OC** is **Not Strongly Light Absorbing (Only Scattering)** and **Semi-Volatile**

- **Important Source of Brown Carbon? (Absorption highly skewed towards UV)**

Dynamic Nature of Fires: Combustion Phases

Flaming Phase: hot and dark; high combustion efficiency

Waterfall Fire (Near Carson City, NV; 14-July-2004)

Smoldering Phase: not-so-hot and white; low combustion efficiency

- Optical Properties
- Size Distribution
- Emission Factors

} Phase Specific

Wet Fuels: (Contain high fuel moisture)

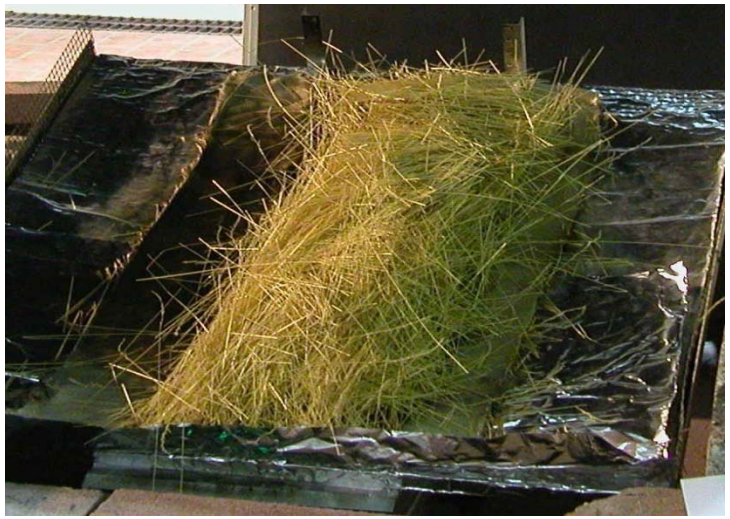

Montana Grass

Alaskan Tundra Cores

<u>Smoldering phase of combustion:</u>

Smoldering is a slow, low-temperature, flameless form of combustion, sustained by the heat evolved when oxygen diffuse to the surface and directly attacks the surface of a condensed-phase fuel.

Potential Mechanism of Particle Emissions

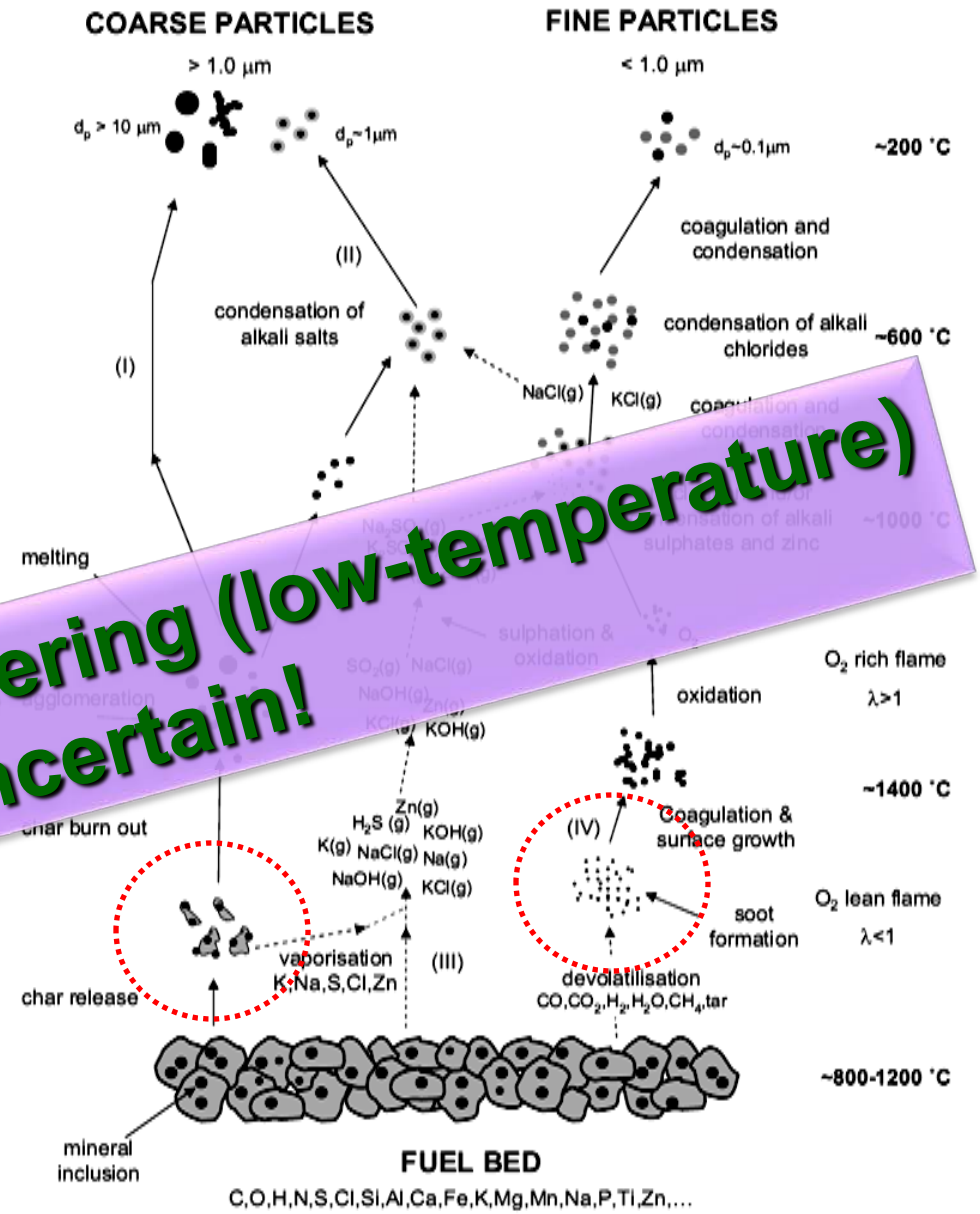

Mechanisms for smoldering (low-temperature) particle emission is uncertain!

Wiinikka (2005);
Bockhorn (1994);
Heible et al. (2000)

Experimental Set-up and Analysis

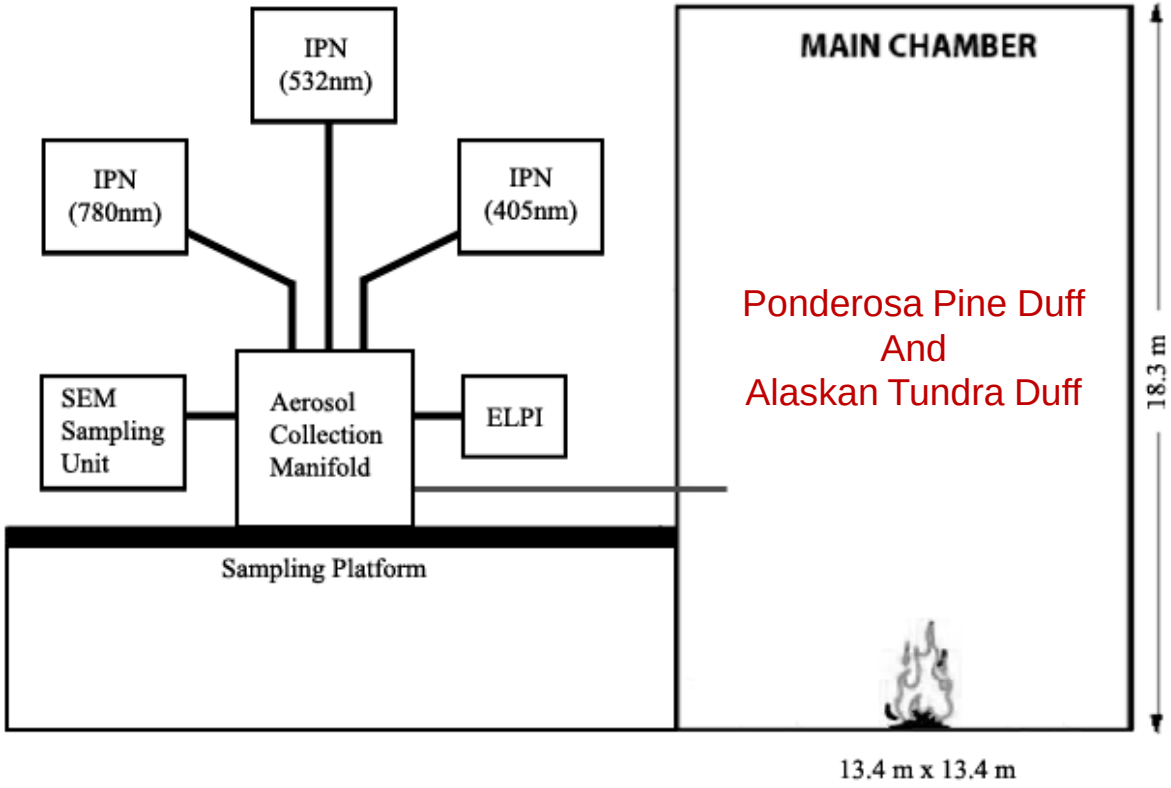

Chamber combustion facility of the United States Department of Agriculture Forest Service Fire Sciences Laboratory (FSL)

Experimental Set-up and Analysis

Integrated Photoacoustic Nephelometer

Absorption Coefficient (Photo Acoustic Spectrometer)

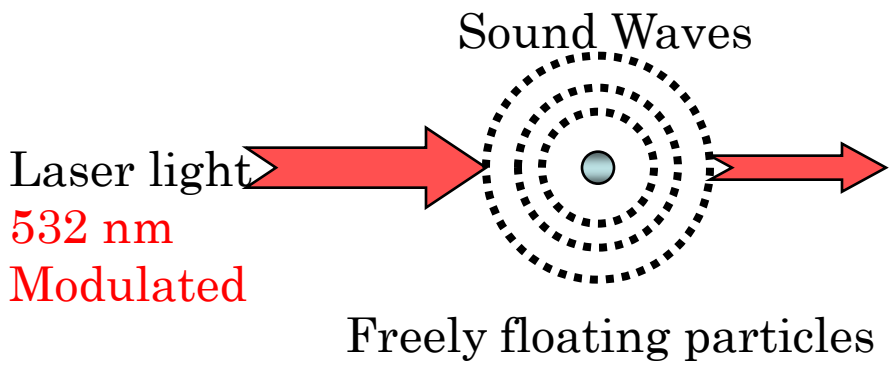

Extinction – Scattering Coefficient (Nephelometer)

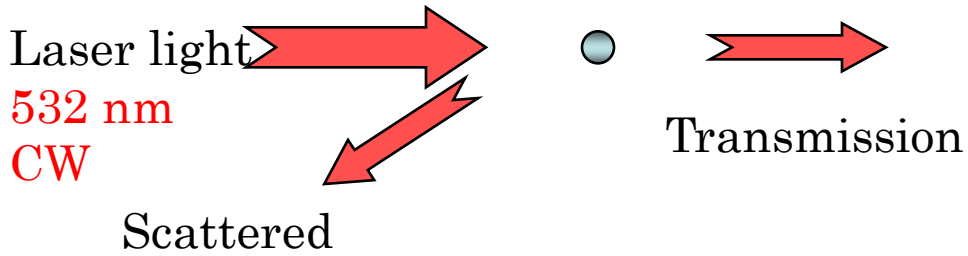

Experimental Set-up and Analysis

SEM analysis for aerosol morphology

Filter coated with a 1-nm thick platinum

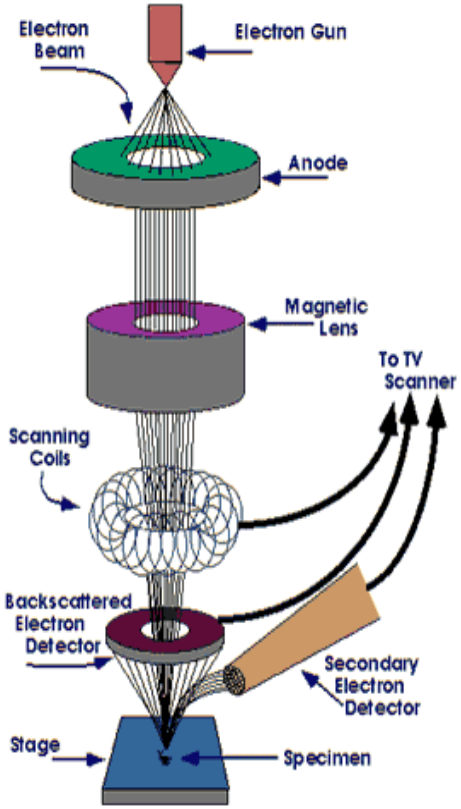

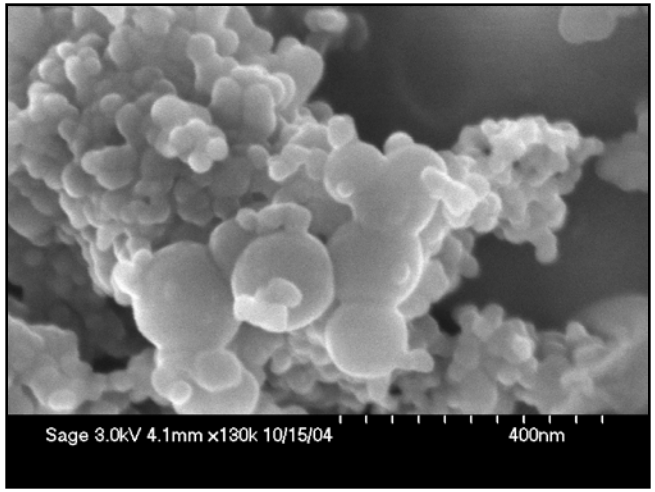

2-dimensional Structural properties

Experimental Set-up and Analysis

Size Distribution Retrieval from ELPI

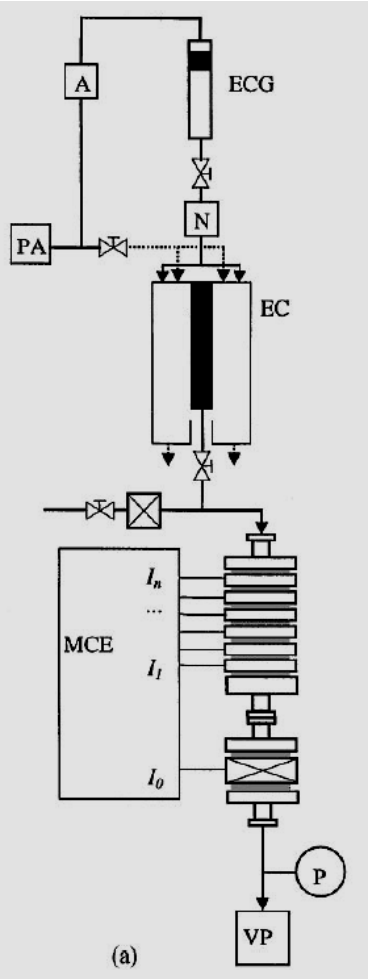

$$I_i = \int_{D_{p,\min}}^{D_{p,\max}} k_i(D_p) E_{\mathrm{ch}}(D_p) f(D_p) dD_p$$

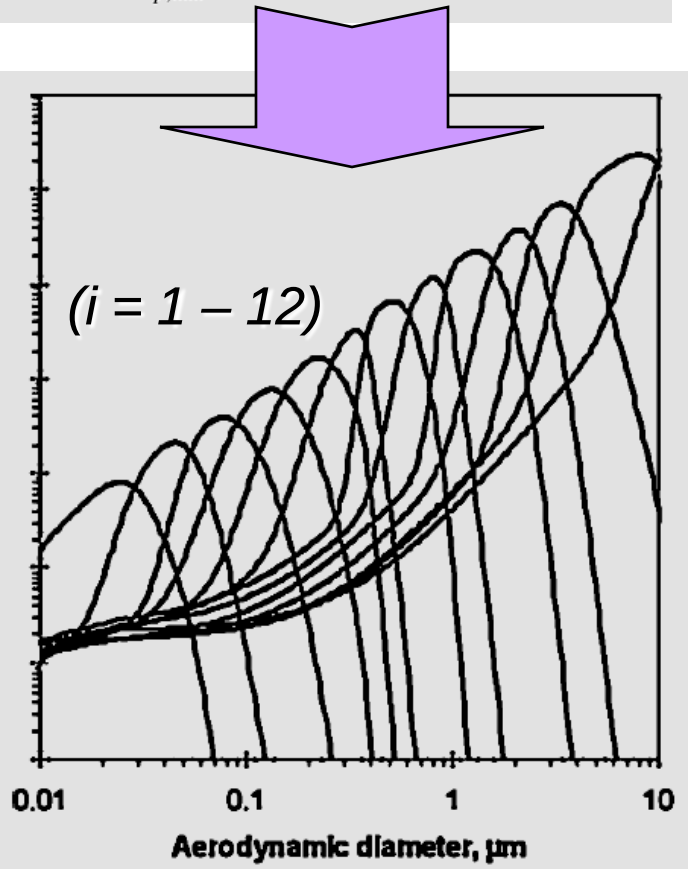

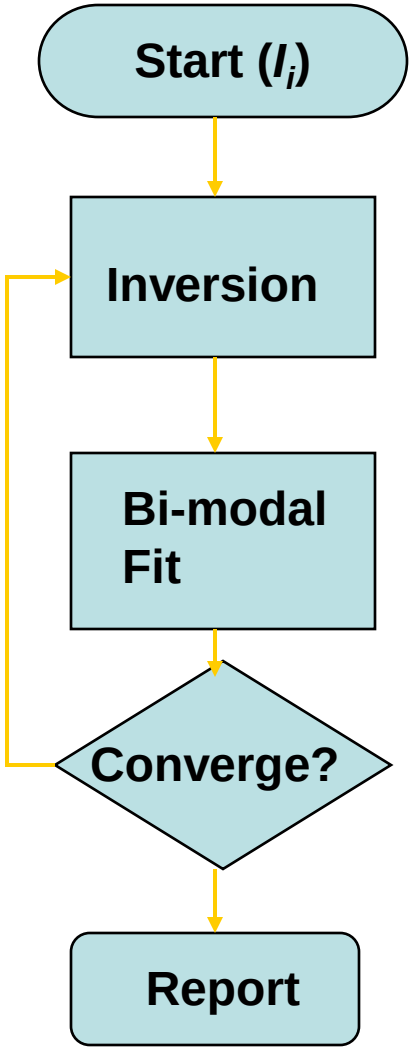

Marjamäki et al. (2005, *AS&T*)

Experimental Set-up and Analysis

Particle Optical Properties Change with Time and the Combustion Phase

Even in chamber burns one observes changes in size distribution with time

For this experiment, all instruments were operated in synchronization for:

2 minutes - Ponderosa Pine Duff

4 minutes – Alaskan Tundra Duff

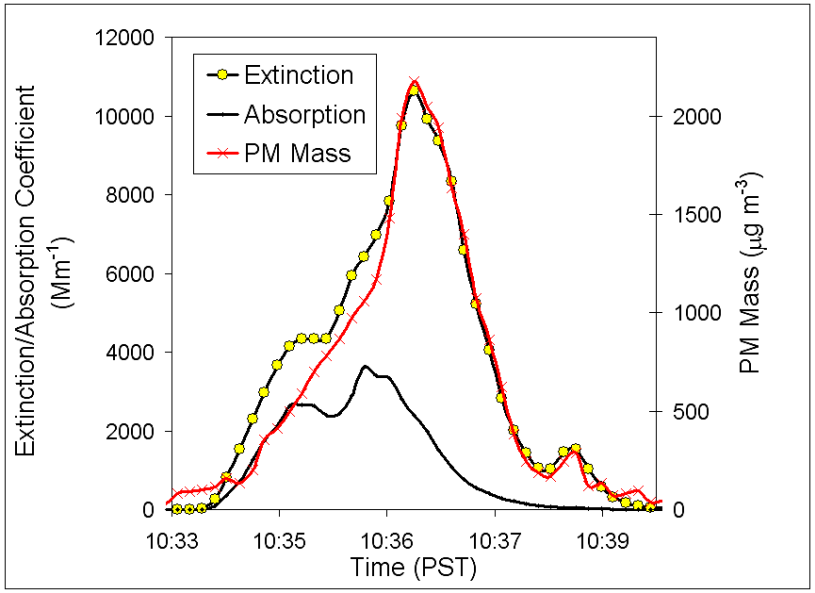

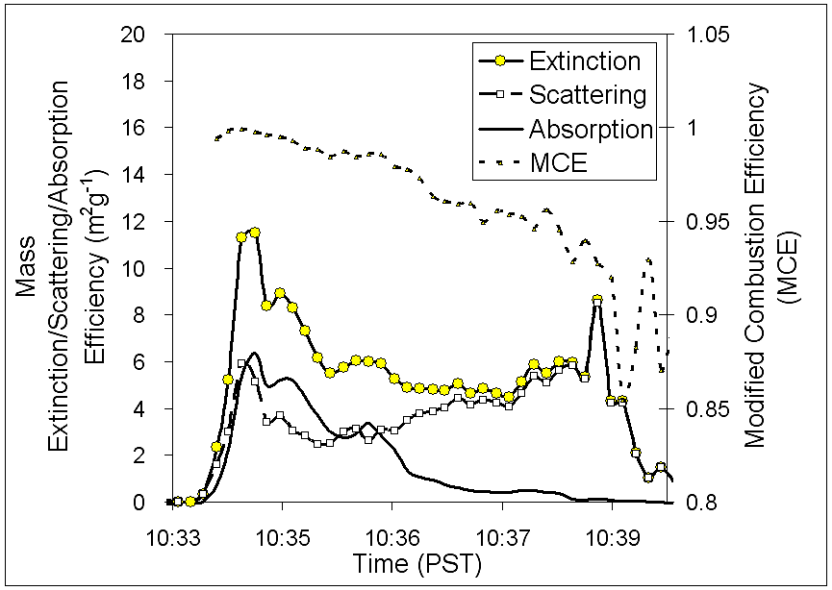

Results and Discussion

Near-Spherical Tar Balls Dominate in the Two Burn Particles

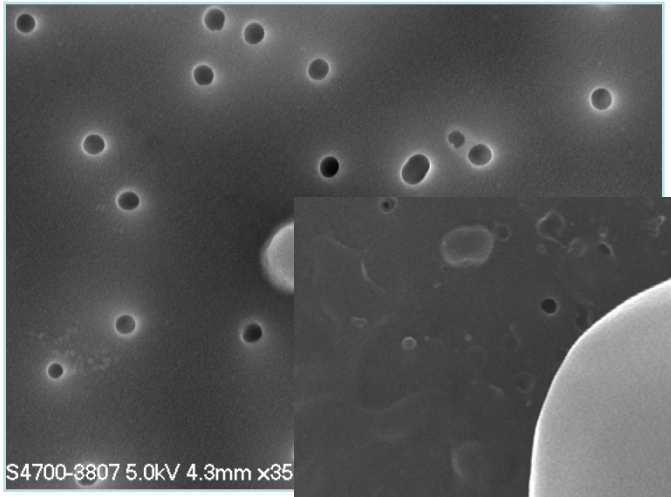

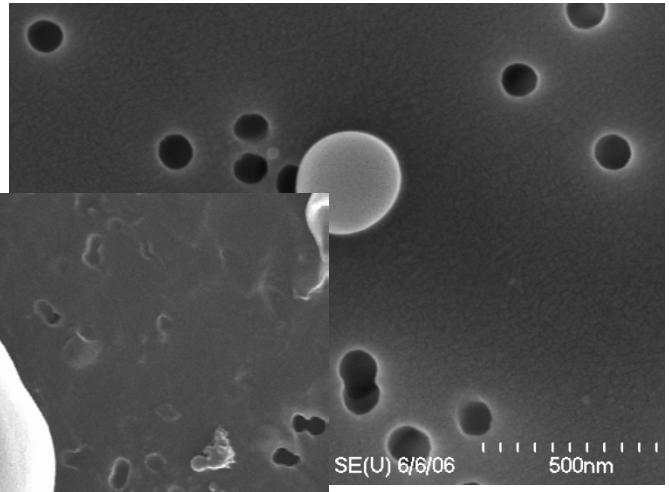

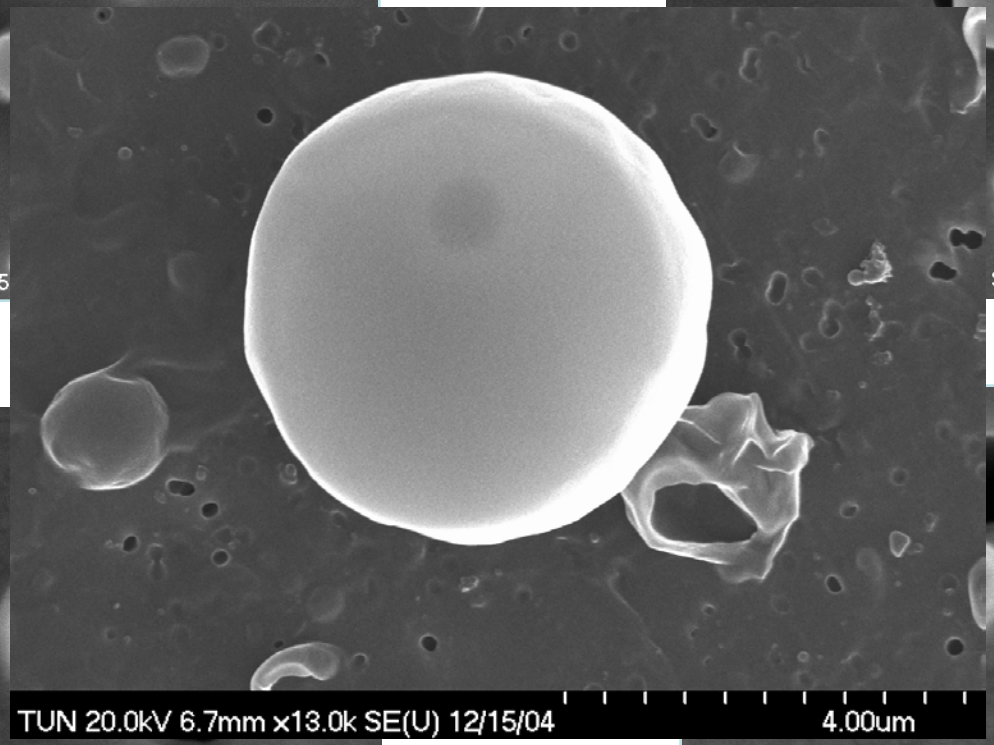

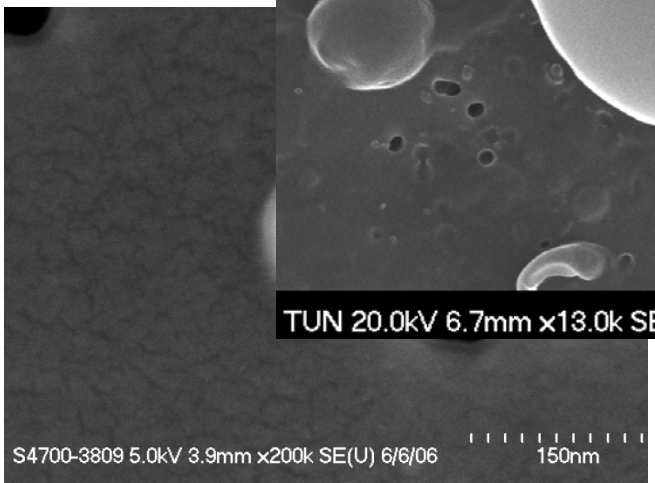

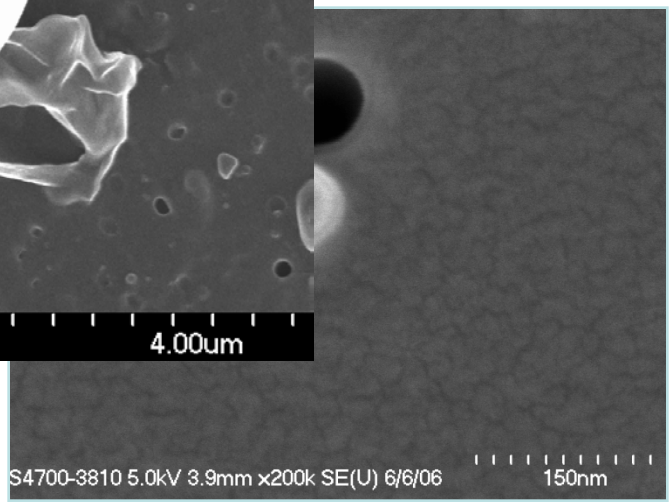

Results and Discussion

Two Pure Smoldering Combustion (Alaskan Tundra & Ponderosa Pine Duff)

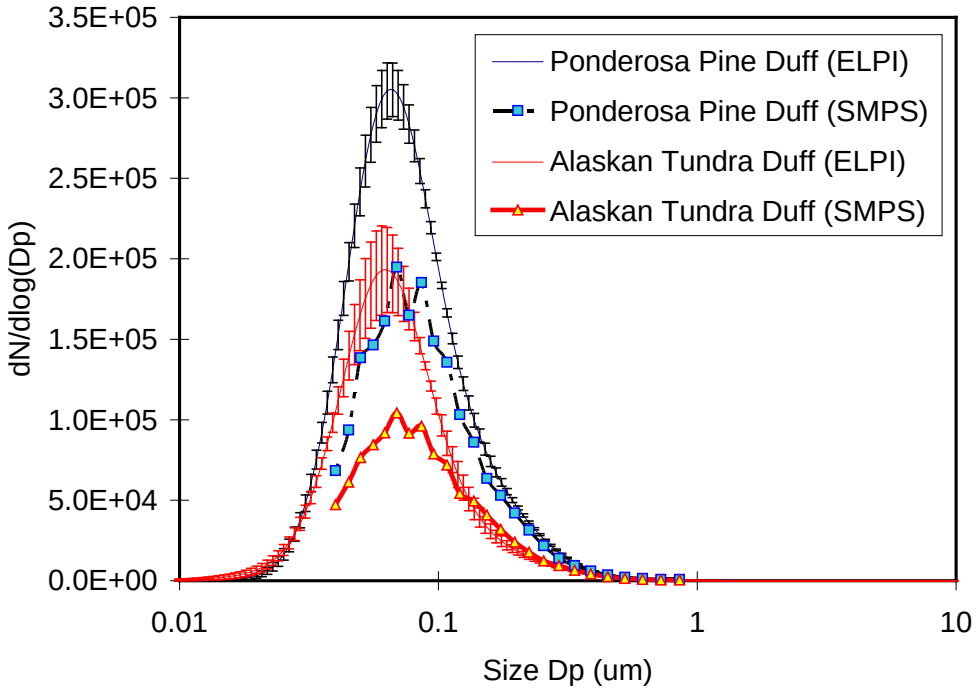

λ	B_{sca}	B_{abs}	Refractive index		λ	B_{sca}	B_{abs}	Refractive index	
			Real	Imag				Real	Imag
405	1134	51.6	Tundra		405	1921	141.6	Pine	
532	893	9.25			532	1544	43.5		
870	876.5	3.5		?	870	1641	15.85		?

Results and Discussion

Can we use the Lorentz Mie theory?

•The near-spherical shape of the particles justifies the use of Mie-theory.

•The Mie code was used for the inverse retrieval of the complex index of refraction (*similar to Guyon et al. 2003*)

•Using the measured particle binned number size distribution, the Mie code first takes the refractive index of water (1.33–0i) and calculates the corresponding scattering and absorption coefficients.

•These values are then compared to the time-averaged values of the measured scattering and absorption coefficients and the real and imaginary part of the refractive index are then increased stepwise until the calculated and measured optical coefficients agree to within 0.5%.

Results and Discussion

Optical Properties

Fuel Name	*B_{sca} & B_{abs} (Mm^{-1}) 405nm*	*B_{sca} & B_{abs} (Mm^{-1}) 532nm*	*B_{sca} & B_{abs} (Mm^{-1}) 780nm*	*Refractive Index 405 nm*	*Refractive Index 532nm*	*Refractive Index 780 nm*
Ponderosa Pine Duff	N/A	1524 & 63.2	721.6 & 21	N/A	1.73 + .0031i	1.59 + .0019i
Alaskan Duff	1150 & 56	906.5 & 9.7	467 & 3.9	1.83 + 0.0076i	1.75 + 0.0019i	1.60 + 0.0014i

Real Part : 1.83 (405nm) - 1.60 (780nm)

Imaginary Part: 0.0076 (405nm) - 0.0014 (780nm)

Absorption Angstrom Coeff: ~6.5 (405-532nm) and ~2.4 (532-780nm)

Single Scattering albedo: >0.90

Chakrabarty et al. 2008, to be submitted to GRL

Results and Discussion

Uncertainty in the Calculations

A sensitivity study was performed where uncertainty in the different individual parameters – scattering and absorption coefficient (~5), and the ELPI size retrieval (~15%) – were individually varied, and the so calculated refractive index was compared with the original one.

Using the method of quadrature sum of the individual errors, the measurement errors in the real part of the index of refraction were calculated to be around 4.1% and that in the imaginary part were approximately 13.6%.

Results and Discussion

	Absorption Angstrom Exponent (405 – 532 nm)	Real Refractive Index (532 nm)	Imaginary Refractive Index (532 nm)
Alaskan Duff	6.5	1.75	0.002
Ponderosa Duff	N/A	1.72	0.003
HULIS (Hoffer et al. 2006)	~7 (300-700nm)	~1.7	0.0016 – 0.0019
Soot/BC (Bond & Bergstrom, 2006)	0.9 - 1	1.5 – 2	0.4 – 1

Category 1	C/O	%sp^2
Ponderosa Pine Needles	70/30	32
Ponderosa Pine Duff	87/13	40
Alaskan Tundra Core Duff	82/18	25
Southern Pine Needles	69/31	44
Ceanothus (I)	78/22	31
	Mean 77/23	Mean 34
Category 2		
Rice Straw (I)		49
Puerto Rico Fern (dry) (I)	74/26	56
Puerto Rico Mixed Woods	80/20	60
Palmetto (I)	77/23	48
	Mean 77/23	Mean 53
Category 3		
Chamise (I)	80/20	81
Utah Juniper Foliage & Stick (I)	91/9	82
Utah Sage Rabbit Brush (I)	84/16	86
	Mean 85/15	Mean 83
Soot Standard		
Methane Soot	84/16	79

STXM/NEXAFS by Mary Gilles group at LBNL

Hopkins et al. 2007 GRL

Results and Discussion

EC/TC Ratio

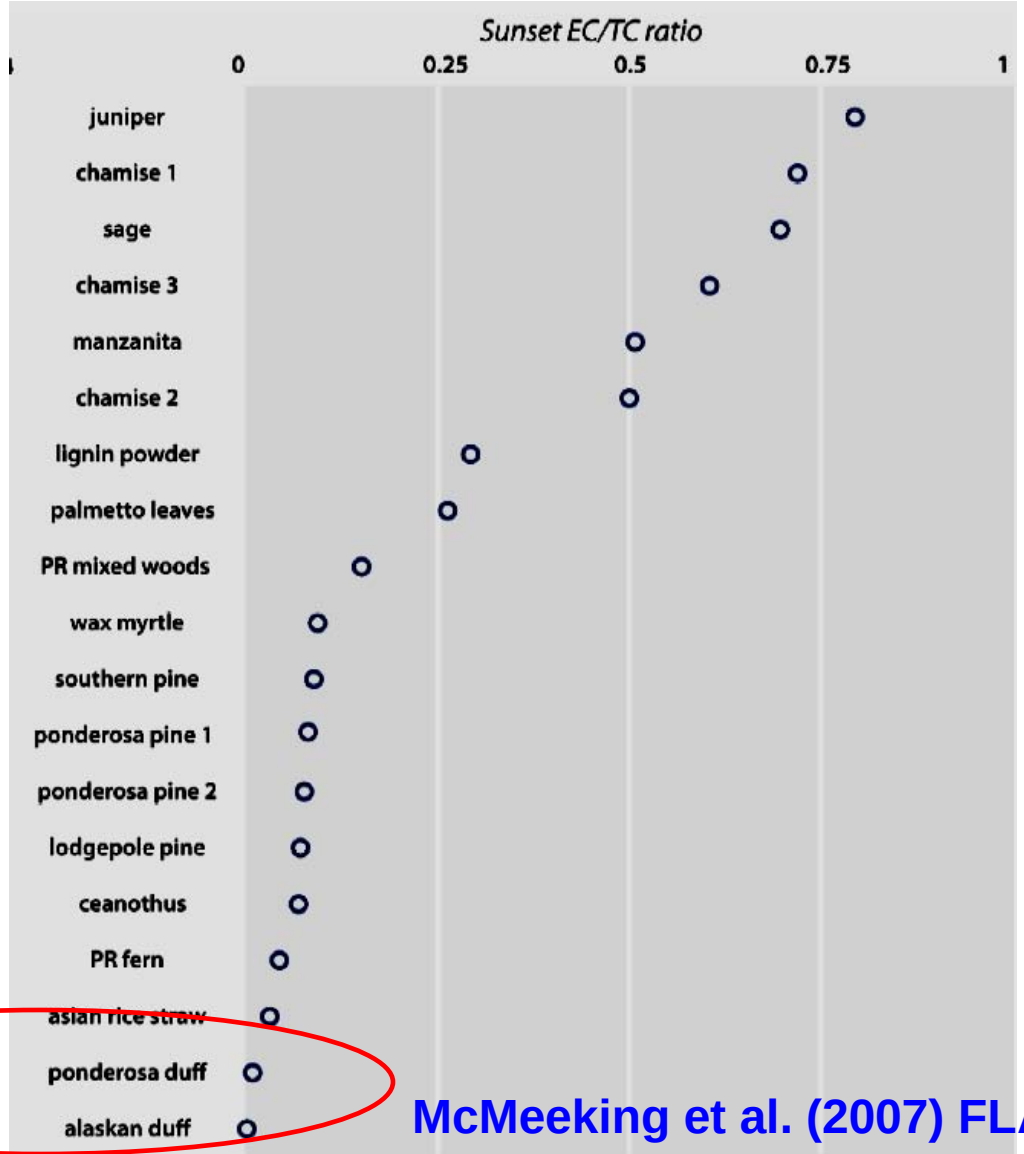

Thermal Optical Measurements

McMeeking et al. (2007) FLAME (Do not cite)

Summary

- Optical properties of carbonaceous aerosol ("tar balls") emitted from the smoldering combustion of two high-moisture-content fuels - Ponderosa Pine Duff and Alaskan Duff

- On average, the complex index of refraction of the particles ranged between 1.83 + 0.0076i (405nm) and 1.6 + 0.0014i (780nm).

- High angstrom coefficient of absorption (~6.5) was observed between wavelengths 405nm and 532 nm for these particles suggesting the possibility of HULIS as the primary aerosol component in tar balls.

- Significant fraction of these tar balls reside in the atmosphere might help partially explain for the up to now unexplained anomalously high fraction of light absorption observed in the troposphere

Acknowledgement

nps.gov

National Park Service
U.S. Department of the Interior

USDA United States Department of Agriculture

National Science Foundation
WHERE DISCOVERIES BEGIN

Thank you for your attendance!!

(M)any Questions??